

Deactivating Chemical Agents Using Enzyme-Coated Nanofibers Formed by Electrospinning

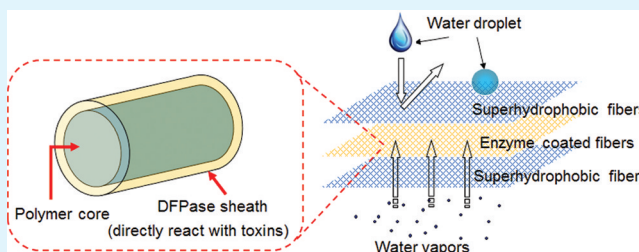
D. Han,[†] S. Filocamo,[‡] R. Kirby,[‡] and A. J. Steckl^{*,†}

[†]Nanoelectronics Laboratory, University of Cincinnati, Cincinnati, Ohio 45221-0030, United States

[‡]Biological Science and Technology Team (BSTT), Natick Soldier Research Development and Engineering Center, Natick, Massachusetts, United States

ABSTRACT: The coaxial electrospinning technique was investigated as a novel method to create stabilized, enzyme-containing fibers that have the potential to provide enhanced protection from chemical agents. Electrospinning is a versatile technique for the fabrication of polymer fibers with large length (cm to km): diameter (nm to μm) aspect ratios. The large surface to volume ratios, along with the biofriendly nature of this technique, enables the fabrication of fiber mats with high enzyme concentrations, which amplify the catalytic activity per unit volume of membrane. Blended composite (single-source) fibers incorporate enzyme throughout the fiber, which may limit substrate accessibility to the enzyme. In contrast, core/sheath fibers can be produced by coaxial electrospinning with very high enzyme loading (>80%) in the sheath without noticeable loss of enzymatic activity. Several core–sheath combinations have been explored with the toxin-mitigating enzyme DFPase in order to achieve fibers with optimum properties. The concentration of fluoride released, normalized for the amount of protein incorporated into the sheath, was used as a measure of the enzyme activity versus time. The coaxial core/sheath combination of PEO and DFPase produced the highest activity (~ 7.3 mM/mg).

KEYWORDS: coaxial electrospinning, DFPase, enzyme, chemical warfare, nanofiber, decontamination



INTRODUCTION

Chemical warfare agents are a threat to both military and civilian populations. Many of these agents are part of a class of compounds known as organophosphates (OPs); they disrupt the central nervous system through inactivation of esterases such as acetylcholinesterase, and include such toxins as Sarin, Soman, Tabun, and diisopropylfluorophosphate (DFP).^{1,2} Current protocols for effective neutralization of these compounds involve the use of harsh chemicals (e.g., strong base, bleach, or strong oxidants), and in some cases can generate waste almost as harmful as the toxin. Naturally occurring substances specifically tailored to react with OPs would be an ideal choice for protection and decontamination.^{3,4}

Organophosphatases are naturally occurring enzymes that can neutralize OPs. While these enzymes are able to effectively break down OPs, many of them are expensive and environmentally sensitive. Diisopropylfluorophosphatase (DFPase), a reasonably stable organophosphatase produced by squid, has shown broad based activity against OPs. Clones of this enzyme have been produced from bacteria, providing a way to mass-produce this enzyme.⁵ Thus, DFPase is a logical choice to test stabilization methods and their effects on enzyme activity.

Enzymatic Detoxification. Enzyme hydrolysis methods are highly effective in neutralizing DFP and other OP nerve agents. The DFPase enzyme catalyzes the hydrolytic cleavage of the P–F bond in the DFP molecule, releasing diisopropylphosphate (DIP) and fluoride, which do not have the toxicity

of DFP. A calcium ion and an aspartic acid residue (D229) play active roles in the detoxification mechanism; the calcium ion polarizes the fluorophosphate, leaving it susceptible to attack by the carboxylate group, resulting in the release of the fluoride ion.^{6,7}

Electrospinning. Organophosphatases have seen limited application due to their sensitivity to environmental conditions, such as pH, temperature, and humidity. Encapsulation and covalent attachment techniques have been used to stabilize enzymes with some success.^{8–18} However, encapsulation can cause a decrease in activity rate due to diffusion rate effects, and surface attachment can decrease enzyme activity as well as limit the amount of enzyme loading on the material. Previous studies using DFPase have described decreases in enzyme activity of up to 70%.^{19–21} Nanostructures, such as nanoparticles and nanofibers, have attracted much attention due to their extremely high surface to volume ratio (SVR) that can promote the catalytic activity. While the use of nanoparticles has some difficulty with uniform dispersion and recycling,²² nanofibers provide several very attractive aspects: (a) easy handling and recycling; (b) high SVR; (c) large variety of materials; (d) high porosity for easy access on fiber surfaces; (e) multilayer composition.

Received: August 8, 2011

Accepted: November 16, 2011

Published: November 16, 2011

Since electrospinning is a very attractive method for nanofiber production, electrospun nanofibers have been used as a supporting material for enzymes in different ways. The most common approach for enzyme loading on electrospun fibers is the dip-coating method. After a fibrous mat is formed by electrospinning, it is immersed into the enzyme solution for a certain period of time for enzyme adsorption. Cross-linkers^{23,24} can be utilized to add sequential layers of enzyme on the fiber mat. Modifications to the fiber surface^{8,18,25} can be performed to improve the surface chemistry for enzyme attachment and subsequent increased enzyme activity. Another well-known method is to electrospin from a solution containing a blend of enzyme and electrospinnable polymer.^{14,26} Although this method provides a one-step simple route for enzyme loading on fibers, the fraction of the polymer in the solution is quite large in order for the blend to be electrospinnable. Therefore, a relatively small amount of enzyme is present on the fiber surface, leading to lower catalytic activity.

Coaxial Electrospinning. In this report, coaxial electrospinning that produces fibers with a core–sheath structure in one step is compared to single nozzle electrospinning of a polymer and enzyme blend (coelectrospinning). Using coaxial electrospinning, enzymes encapsulated by a biocompatible polymer sheath layer have been reported.²⁷ This approach can be used for controllable drug release systems without an initial burst release. Using electrospinning to form fiber mats with very high SVR allows the incorporated enzyme to interact most efficiently with the chemical agents. The versatility of the coaxial core/sheath electrospinning fiber formation is clearly a key asset in producing the optimum material for protection from chemical toxin exposure. To the best of the authors' knowledge, this article provides the first report of enzyme coated polymer fibers using coaxial electrospinning.

EXPERIMENTAL SECTION

Materials. Crude recombinant diisopropylfluorophosphatase (DFPase) at 40% purity was purchased from Codexis and used without further purification. For the purpose of this paper, the overall material is collectively referred to as DFPase. Poly(ϵ -caprolactone) (PCL) (MW = 80 kDa), piperazine-N,N'-bis(2-ethanesulfonic acid) (PIPES) and diisopropylfluorophosphate (DFP) were purchased from Sigma-Aldrich (St. Louis, MO), and used as received. Fluoride concentration measurements were obtained with an Orion 9609 ionplus fluoride electrode purchased from Thermo Fisher Scientific Inc. (Waltham, MA). Poly(ethylene oxide) (PEO) (MW = 900 kDa) and 2,2,2-trifluoroethanol (TFE, 99.8% purity) solvent was purchased from Acros Organics (Geel, Belgium). These materials were used as received without any further modification.

Fabrication. The coaxial electrospinning method is illustrated in Figure 1a. Solutions for the core and sheath materials are separately fed into the coaxial nozzle from which they are ejected simultaneously. Upon application of a sufficiently high voltage, a compound Taylor cone is formed and a liquid jet is ejected consisting of the core material enveloped by the sheath material. The ejected compound liquid jet experiences whipping and bending instabilities within a sufficient distance for evaporating its solvent thoroughly, and consequently, becomes a solid micro/nanofiber with a core–sheath structure (Figure 1b). Different characteristics from each material can thus be combined into a single fiber. Using the coaxial electrospinning method we have previously explored the formation of specialized fibers for several applications, including tissue engineering,²⁸ superhydrophobic fabrics,²⁹ photocatalytic materials,³⁰ etc.

To demonstrate the versatility of coaxially electrospun DFPase fibers, we also formed DFPase containing fiber mats by alternative methods: (a) electrospinning from various blended solutions resulting

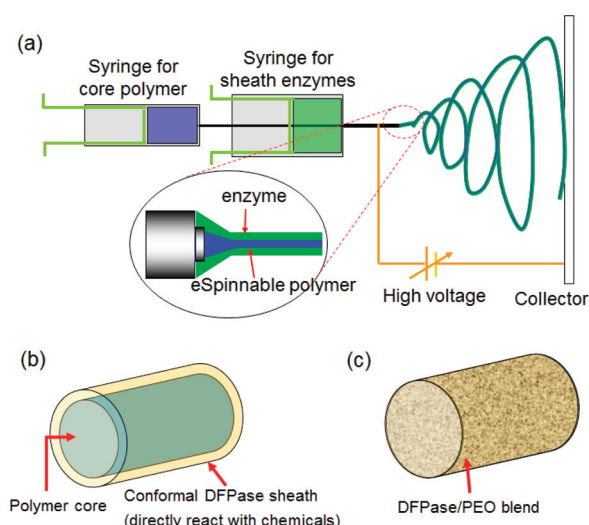


Figure 1. Electrospinning of enzyme containing fibers: (a) coaxial dual solution electrospinning; (b) core–sheath coaxial fiber with polymer core and conformal DFPase containing sheath; (c) uniform DFPase/PEO blended fiber using single solution electrospinning.

in fibers with uniform blend compositions (Figure 1c) and (b) dip-coating fiber mats into DFPase solution.

Enzyme Blended Electrospinning. Most enzymes are not directly electrospinnable because of low viscosity (even at very high concentrations). To facilitate the electrospinning of enzymes, the most convenient method is to form solutions with electrospinnable polymers. When the solution contains a large portion of electrospinnable polymer, the resulting fibers have a relatively small portion of enzyme exposed at the fiber surface since a significant amount of the enzyme is embedded within the fiber. To optimize the amount of viable enzyme, and therefore increase catalytic efficiency of the blend fiber approach, one needs to determine the minimum polymer concentration required for uniform fiber production.

Blended solutions for the electrospinning were prepared by dissolving DFPase (3 wt.%) and PEO (3 wt.%) into DI water. Sodium dodecyl sulfate (SDS) surfactant was added at 0.05 wt.% not only to reduce the surface tension of the aqueous blended solution but also to provide a weakly basic environment for the enzyme solution. A high voltage of 20 kV was applied over a 20 cm gap distance and a solution flow rate of 0.4 mL/h was used. The solution contained equal amounts by weight of DFPase enzyme and PEO polymer. A total solution amount of 670 μ L was dispensed.

Enzyme Coaxial Electrospinning. Two polymers were utilized in coaxial electrospinning experiments: water-soluble PEO, and PCL that is not water-soluble and requires select organic solvents. Coaxial electrospinning conditions are summarized in Table 1. DI water was used as the solvent for PEO and DFPase and chloroform was used for the PCL solution.

The total dispensed amount of polymer in the various samples was maintained roughly constant. Table 2 summarizes the compositions and weights of the 9 types of fiber mats fabricated: the weight of fiber mats, the weight ratio of polymer to DFPase and the amounts DFPase loaded for each sample type.

Dip-Coating Method. PCL-only fiber mats were dip-coated into a 3.3 wt % DFPase aqueous solution. After 5 min of immersion, the dip-coated fiber mats were lightly blotted and dried at room temperature overnight.

Enzyme Activity Measurement. The ability of electrospun DFPase to defluorinate DFP was measured based upon a previously described method with a fluoride probe.^{21,31} Briefly, samples were added to a glass Petri dish with 7.00 mL of 10–25 mM PIPES buffer, pH 7.2 and a stir bar. The samples were allowed to equilibrate for 3 min under the reference and fluoride electrodes. DFP solutions were prepared in Milli-Q deionized water at a concentration of 0.010 M.

Table 1. Coaxial Electrospinning Conditions for Coaxial Fiber Mats: High DFPase Loading (Figure 5) and Low DFPase Loading (Figure 8)

figure	description (wt % in solution)	distance (cm)	applied voltage (kV)	flow rates (mL/h) core and sheath
5	PEO(4) core & DFPase(10) sheath	20	13–13.5	0.9 and 0.2
	PEO(4) core & DFPase(4)/PEO(1)/SDS(1) sheath	20	12	0.6 and 0.2
	PCL(10) core & DFPase(4)/PEO(1)/SDS(1) sheath	20	11–12.6	0.5 and 0.2
8	PEO(4) core & DFPase(1)/SDS(0.1) sheath	20	12.5	1.2 and 0.1
	PEO(4) core & DFPase(1)/PEO(2)/SDS(1) sheath	20	13–13.5	0.8 and 0.1
	PCL(10) core & DFPase(1)/PEO(2)/SDS(1) sheath	20	13–15	0.5 and 0.25

Table 2. Summary of Material Compositions for Electrospun Fiber Mats: High DFPase Loading (Figure 5) and Low DFPase Loading (Figure 8)^a

figure	description	wt ratio (polymer: DFPase)	fiber mat weight ^b (mg)	DFPase amount ^b (mg)
5	DFPase dip coated PCL fibers	13:1	44.19	3.02
	PEO/DFPase blended composite fibers	1:1	34.91	17.46
	coaxial fibers (PEO core & DFPase sheath)	1.8:1	21.83	7.80
	coaxial fibers (PEO core & DFPase/PEO sheath)	3.25:1	26.43	5.87
	coaxial fibers (PCL core & DFPase/PEO sheath)	9.31:1	23.95	2.57
8	coaxial fibers (PEO core & DFPase sheath)	48.1:1	24.86	0.52
	coaxial fibers-R (PEO core & DFPase sheath)	48.1:1	24.4	0.52
	coaxial fibers (PEO core & DFPase/PEO sheath)	34:1	20.59	0.57
	coaxial fibers (PCL core & DFPase/PEO sheath)	30.9:1	12.63	0.38

^aEstimated based on experimental conditions such as solute concentration, solution density, and flow rates. ^bApparent area: 4 in.²

Once equilibrated, a 3.00 mL aliquot of the DFP solution was added, and fluoride ion measurements were recorded every 5 s for 3 min. Controls were also established for comparison: (1) a 3.00 mL aliquot of DFP solution was added to 7.00 mL of PIPES buffer and monitored for 3 min, to determine the rate of self-degradation; (2) DFPase was added to 7.00 mL of PIPES buffer, allowed to equilibrate; (3) 3.00 mL of DFP was then added and monitored as described.

RESULTS AND DISCUSSION

The core–sheath structure of the coaxially electrospun fibers was demonstrated by TEM and fluorescence microscopy. TEM observation in Figure 2a shows the core–sheath structure. The core and fiber diameters are 114 and 128 nm, respectively, and the wall thickness is ~ 7 nm. This is well matched with our quantitative analysis considering material densities and flow rate ratio, which results in a calculated ratio of core radius to fiber radius of $\sim 1:1.1$. For fluorescence microscopy, we have added a Keystone Red XB dye to the sheath DFPase solution. Keystone Red dye is soluble in the aqueous sheath solution, but not in the PCL core solution. Fibers formed in this manner exhibited strong red fluorescence, as shown in Figure 2b. To confirm the location of the dye in the sheath, we immersed the fibers in water for 3 h followed by rinsing with running water. Red fluorescence was not observed in the rinsed fiber mat (Figure 2c). At the same time no noticeable change was observed in the

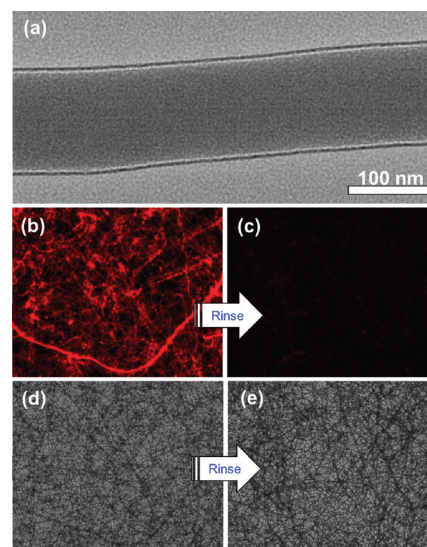


Figure 2. (a) Core–sheath structure observation using TEM; and fluorescence microscopy of coaxial fibers containing Keystone Red dye in the sheath, before and after rinsing with water: (b) initial dark-field image, (c) dark-field image postwashing, (d) initial bright-field image, (e) bright-field image postwashing. Exposure times for bright-field and dark-field modes are 2 ms and 2 s, respectively.

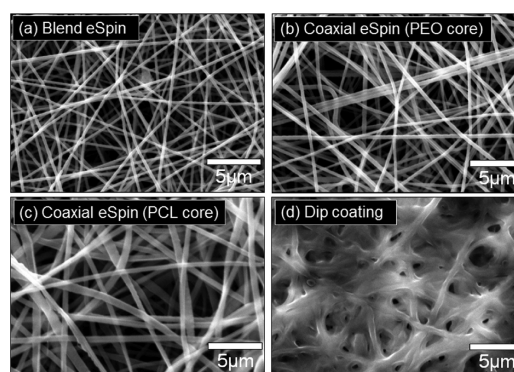


Figure 3. SEM observations of electrospun fibers (a) PEO & DFPase blend fibers with 1:1 wt. ratio; coaxial fibers with DFPase sheath and (b) PEO core; (c) PCL core; (d) PCL fibers dip-coated with DFPase solution.

overall morphology of the fiber mat as can be seen in the bright-field photographs taken before and after rinsing (Figure 2d, e). Therefore, it appears that the coaxially electrospun fibers have a core–sheath structure with a DFPase/dye sheath layer and a PCL polymer core.

Fiber morphologies have been observed in more detail using an EVEX mini-SEM, SX-3000. As shown in Figure 3a–c, the coaxial and blended fibers provide good porosity, as there are

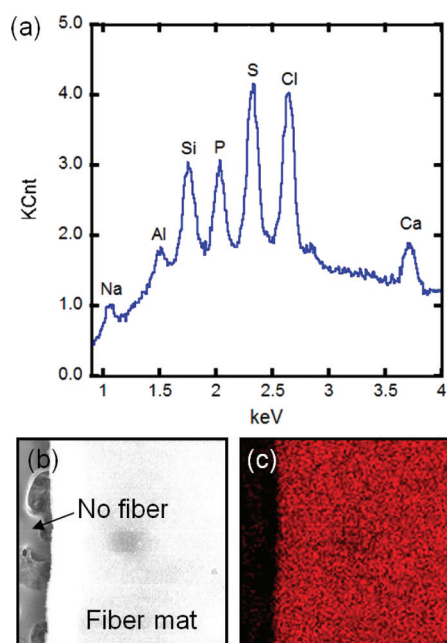


Figure 4. Chemical composition analysis of PEO–DFPase coaxial fiber mat: (a) EDX spectrum, (b) SEM image, (c) element map of sulfur.

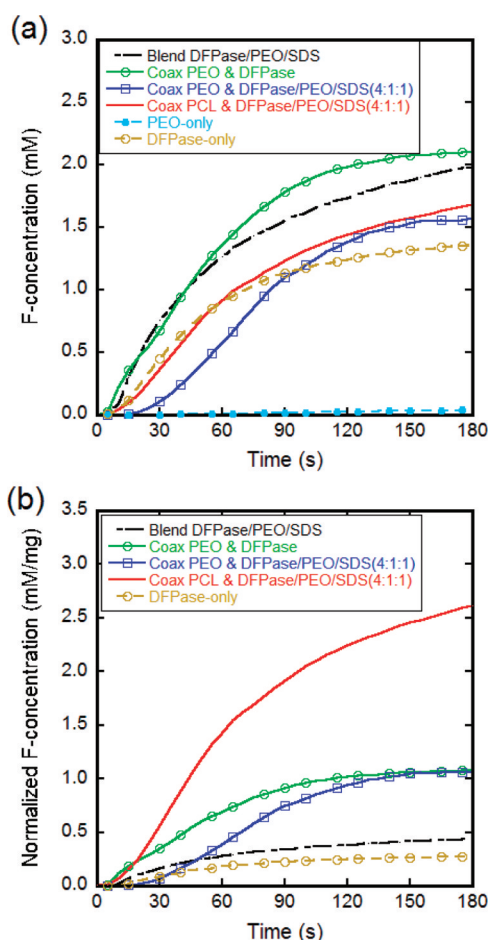


Figure 5. Enzymatic activity for detoxifying DFP agent through reaction with DFPase: (a) released F concentration vs time; (b) released F concentration normalized to amount of initial enzyme incorporation vs time.

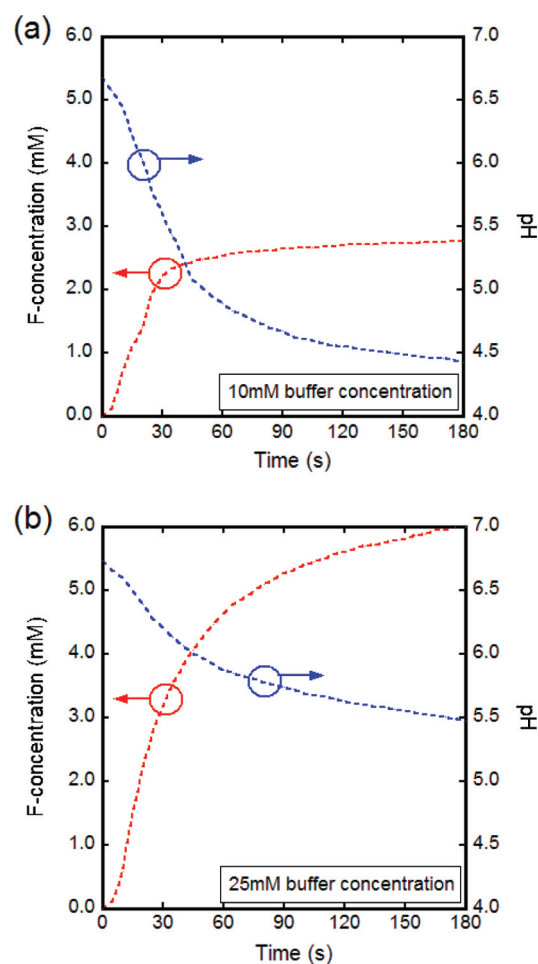


Figure 6. Dependence of DFP–DFPase reactions on pH change in solution: 2.5 mg of DFPase added in 10 mL of PIPES buffered DFP solution made of 3 mL of 25 mM DFP solution and 7 mL of (a) 10 or (b) 25 mM PIPES buffer solution. Measurement repeated 3 times and averaged graphs are shown.

no filled pores or interdiffused fibers. In contrast, the porosity of the dip-coated PCL fiber mat shown in Figure 3d was significantly decreased by loading of the DFPase. Additionally, blended composite fibers (Figure 3a) and coaxially electrospun fibers (Figure 3b, c) show uniform fiber morphology without beads.

For the dip-coated fiber mat, as shown in Figure 3d, the total surface area was decreased by the reduced porosity and DFPase was not loaded uniformly over the entire PCL fiber mat, especially when the PCL fiber mat was thick. On the other hand, for fibers formed by coaxial or blend electrospinning, the amount of DFPase enzyme can be manipulated by adjusting concentration and/or flow rates without sacrificing fiber mat porosity and uniformity. Therefore, the dip-coating technique was not pursued in further studies.

The chemical composition of coaxial fiber mats has been investigated using energy dispersive X-ray analysis, as shown in Figure 4. In contrast to PEO fibers, PEO–DFPase coaxial fibers (Figure 4a), show additional peaks for sodium, silicon, sulfur, chlorine, and calcium. DFPase includes numerous sulfur-containing amino acids in its structure. Since sulfur is not present in any of the polymers used, we chose it for elemental mapping in order to show the dispersion of DFPase throughout the fiber mats. As shown in panels b and c in Figure 4, the

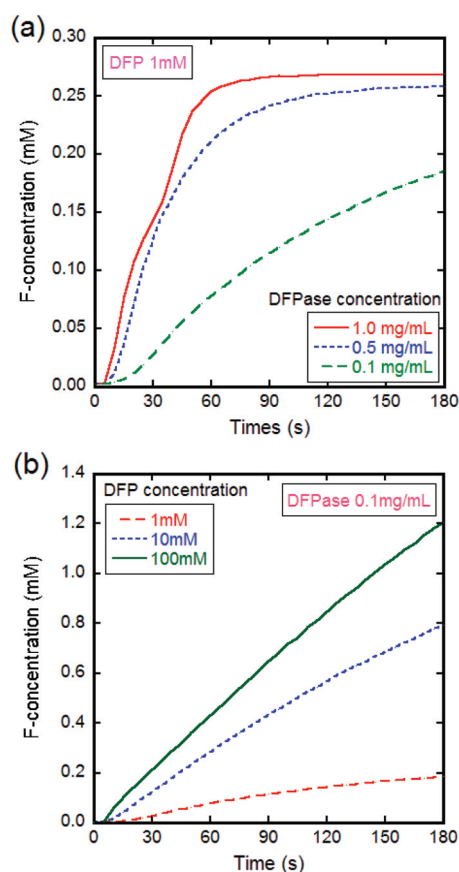


Figure 7. Reaction kinetics: (a) DFPase concentration effect at 1 mM DFP; (b) linear kinetics at different DFP concentrations with 0.1 mg/mL DFPase concentration.

coaxial fiber mat shows very strong sulfur content, whereas the nonfiber area exhibits only noise level detection. It is clear that the DFPase exists uniformly over the entire fiber mat without any localized large clusters of DFPase.

Catalytic activity of DFPase enzymes has been characterized by measuring the fluoride concentration ($[F]$), which is a product of the hydrolysis reaction with DFP. Initial experiments were carried out to confirm the activity of the enzyme incorporated into electrospun fibers. For this purpose a relatively large amount of DFPase was introduced into the electrospun fiber mat. Figure 5a shows $[F]$ as a function of time for the 6 types of fiber mats described in Table 1, as well as two reference samples: a DFPase-only (no fibers) sample and a fiber-only (PEO) sample. The DFPase-only sample produced a similar amount of $[F]$ to that generated by the DFPase-containing fibers. As expected, the PEO-only sample showed only a trace $[F]$. Further insight into the differences between fiber types was obtained by studying the $[F]$ normalized to the DFPase amount introduced into each sample type. As shown in Figure 5b, the coaxial fiber sample with PCL core and DFPase/PEO sheath has the fastest reaction rate and highest level of $[F]$ released per weight of initial DFPase. Among the fiber mats, the sample with uniform fibers of a blend of DFPase and PEO (1:1 wt. ratio) shows the lowest level of normalized $[F]$ release. Interestingly, the DFPase-only sample exhibited an even lower sensitivity.

All samples show a similar $[F]$ vs time, with a relatively linear initial region followed by saturation to roughly the same $[F]$ value after ~ 2 min. Given that the samples had varying DFPase

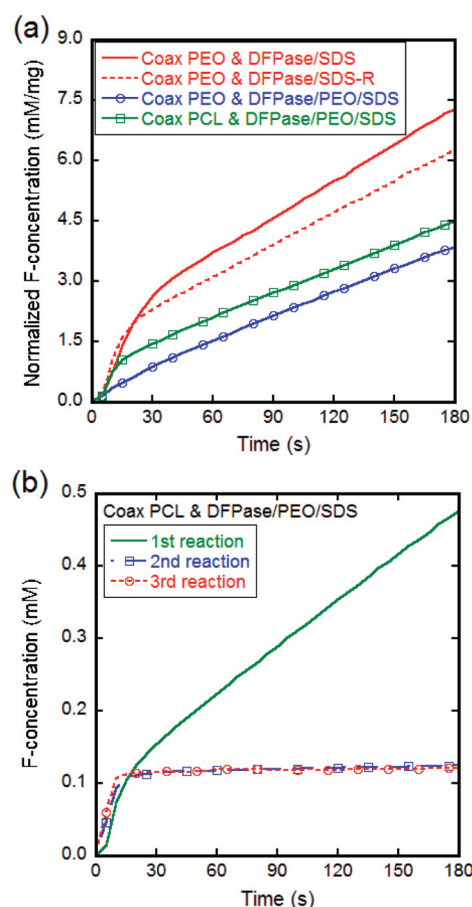


Figure 8. DFP-DFPase linear kinetics: (a) normalized $[F]$ concentration from several coaxial fiber mats; (b) three sequential exposures of coaxial fibers with a PCL core to fresh DFP solutions.

Table 3. Summary of Electrospun Fiber Mats with Linear DFPase-DFP Kinetics^a

#	description	fiber diameter (nm)	surface area ^b (cm ²)	maximum activity ^c $[F]/\text{DFPase}$ (mM/mg)
1	coaxial fibers (PEO core & DFPase sheath)	120 ± 27	8.3 × 10 ³	7.28
2	coaxial fibers-R (PEO core & DFPase sheath)		<20	6.26
3	coaxial fibers (PEO core & DFPase/PEO sheath)	126 ± 33	6.2 × 10 ³	3.86
4	coaxial fibers (PCL core & DFPase/PEO sheath)	218 ± 41	1.3 × 10 ³	4.51

^aEstimated based on experimental conditions such as solute concentration, solution density, and flow rates. ^bApparent area: 4 in.². ^cApparent area: 1 in.².

amounts (from ~ 2.5 to 18 mg) it is clear that the saturation effect is caused by other factors. The most likely explanation is that at these levels of DFPase and DFP, an excess amount of acid is quickly generated. This overwhelms the buffering capacity of the solution, causing a drop in pH. In turn, this deactivates the enzyme by protonation of the active site during hydrolysis. A reduction in pH is known to reduce the DFPase-DFP reaction rate.³² Figure 6 shows both the $[F]$ generated by DFP-DFPase reaction and the pH of the solution as a function

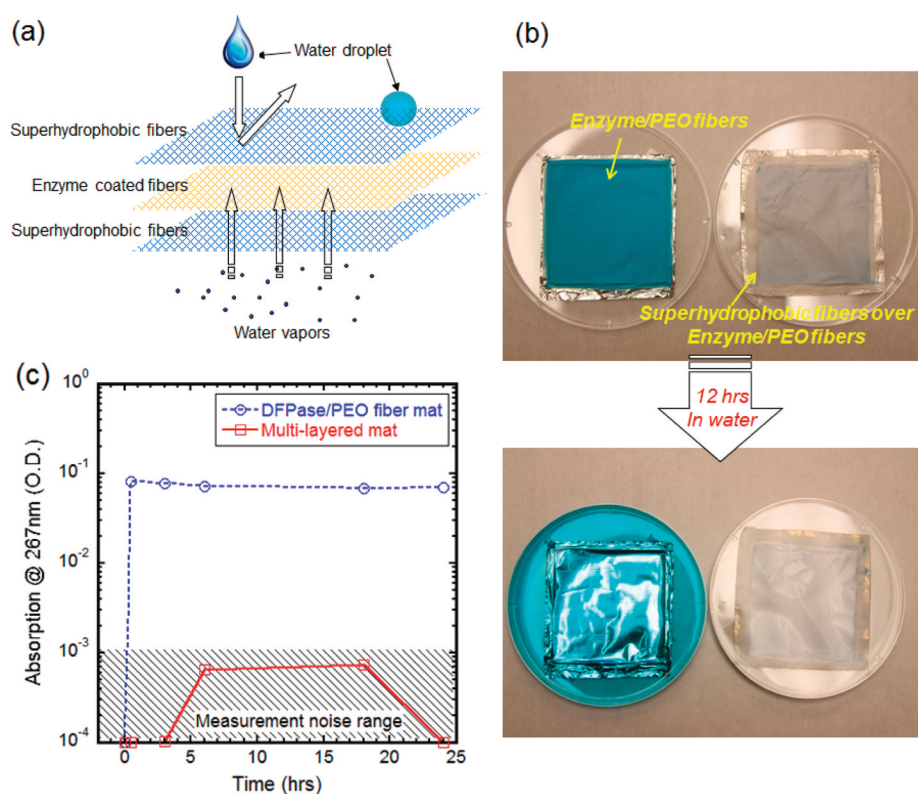


Figure 9. Multilayer fiber mat with outer superhydrophobic fibers and inner enzyme containing fibers: (a) schematic of multilayer fiber mat; (b) demonstration of multilayer protection of enzyme containing fibers; (c) absorption (at peak wavelength ~ 267 nm) vs time, comparison between enzyme/PEO fiber mat and multilayer fiber mat.

of time. At first the $[F]$ increases linearly with time while the pH is reduced. However, when the pH has dropped to the 5.5–6.0 range, a saturation in the $[F]$ level begins to occur. This effect is more dramatic at a lower buffer concentration (Figure 6a), with the pH dropping abruptly and enzymatic reaction saturating at a lower $[F]$ level. As shown in Figure 6b, increasing the buffer concentration leads to a slower pH drop and a higher reaction rate level.

Quantitative comparisons of enzyme efficiency were obtained from later experiments (see Figure 8) because of pH decrease during these preliminary measurements. The decrease in pH is known to reduce enzyme activity.³² Therefore, experiments on DFPase-DFP reaction kinetics were carried out to determine optimum reaction conditions and minimize pH effects. Figure 7a shows $[F]$ vs time for varying DFPase concentrations (0.1–1.0 mg/mL) at a fixed DFP concentration of 1 mM. For the two higher DFPase concentrations the $[F]$ signal was essentially the same, indicating that the DFP amount present was limiting the reaction. Reducing the DFPase concentration to 0.1 mg/mL resulted in a lower $[F]$ and had a much reduced pH effect. Therefore, the next step was to investigate higher DFP concentrations while holding the DFPase concentration at 0.1 mg/mL. As shown in Figure 7b, improved linear $[F]$ dependence was obtained for 10 and 100 mM DFP concentrations. Because of the toxicity of DFP, subsequent experiments were carried out with 10 mM concentration to minimize exposure. In addition, to minimize pH effects, we increased the buffer concentration to 25 mM.

These conditions were utilized to produce and test optimized enzymatically active electrospun fiber mats. Figure 8a shows normalized $[F]$ with respect to time for these optimized coaxial

fiber mats. These data were used to determine enzyme activity as a function of these constructs (Table 3). The coaxial core-sheath combination of PEO core and DFPase sheath produced the highest enzyme activity (~ 7.28 mM/mg), with slightly lower activity levels for PCL core-DFPase/PEO sheath and PEO core-DFPase/PEO sheath constructs. It is important to note that the activity values for these optimized fibers have increased by a factor 2–3 from previous fibers (in Figure 5b). To confirm that the enzyme was not affected by the electric field it experienced during electrospinning, we formed a cast film sample by coaxial dispensing with no applied voltage. As can be seen in Figure 8a, this sample (dashed line) has a similar $[F]$ as its fiber counterpart, indicating that there is no reduction in the enzymatic activity due to the electrospinning process, in contrast to other incorporation procedures, where activity can decrease by up to 70% in comparison to free enzyme in solution. Because in our case no reduction in enzymatic activity was observed, a more rigorous kinetic analysis (such as Michaelis Menten kinetics) was not pursued.

PEO fibers are water-soluble; therefore, they can undergo only a single exposure to the DFP solution. Because PCL is not water-soluble, the PCL core-PEO sheath construction was chosen for further experimentation. Fibers were created with DFPase in the sheath, and then exposed to an aqueous DFP solution. The PEO sheath should dissolve after the first exposure, resulting in potential interactions between DFPase and the PCL core. Figure 8b shows $[F]$ vs time for a single coaxial PCL core-DFPase/PEO sheath fiber mat sequentially exposed to fresh DFP solution for a total of three times. It appears from the resulting data that the sheath material is completely dissolved during the first exposure and subsequent

DFP exposures only exhibited a background level of [F]. This is a similar result to that observed with PCL core–DFPase/dye experiments shown in Figure 2. This indicates that a different fiber construction is necessary to achieve a material that can undergo multiple exposures without degradation.

A different approach was pursued in the design of an enzyme containing fiber mat that is also water resistant. A multilayer scheme, shown in Figure 9a, places the region containing the enzyme-coated PEO fibers between two layers of super-hydrophobic Teflon-coated PCL fibers. A comparison between a conventional enzyme fiber mat and the multilayer fiber mat is shown in Figure 9b. The two mats, which also contained a dye in the enzyme solution for visualization purposes, were immersed in water for 12 h. The conventional mat (Figure 9b, left) released the dye immediately upon being immersed, whereas the multilayer mat (Figure 9b, right) completely contained the dye within the mat even after 12 h. The resulting solutions were tested for the presence of DFPase, which has an absorption peak at ~267 nm. As shown in Figure 9c, the release of DFPase is greatly suppressed by the multilayer structure. This is one of many possible constructs that can be designed using this versatile technique. Studies are ongoing to determine the effects of different approaches to enzyme incorporation on enzyme activity.

SUMMARY AND CONCLUSIONS

We have demonstrated a novel fiber mat construct that incorporates a biological material that is active against harmful chemicals. Coaxially electrospun fibers containing DFPase in the sheath and polymer in the core have shown very promising catalytic activity. This process has been optimized to maximize the amount of enzyme (>80%) loaded into the blended sheath layer, while retaining the enzymatic activity. The process is amenable to changes in the polymer makeup of the construct, which provides a means to form reactive fiber mats that would be active over multiple uses, while protecting the sensitive biological material from environmental damage, leading to inactivation. Future efforts will investigate different layering constructs, as exemplified by the enzyme sandwich described above. This would provide increased environmental protection, as well as potential reusability, and therefore can be studied in conditions that simulate those for extended storage. The coaxial DFPase/polymer fiber formation appears to be a very promising approach for the fabrication of mats or fabrics for decontaminating hazardous chemicals and for protecting people and equipment.

AUTHOR INFORMATION

Corresponding Author

*E-mail: a.steckl@uc.edu.

ACKNOWLEDGMENTS

The work at the University of Cincinnati is partially supported by a contract with the Natick Soldier Research Development and Engineering Center.

REFERENCES

- (1) Hoskin, F. C. G. *Science* **1971**, *172* (3989), 1243–1245.
- (2) Hoskin, F. C.; Roush, A. H. *Science* **1982**, *215* (4537), 1255–1257.
- (3) Rogers, J.; Hayes, T.; Kenny, D.; MacGregor, I.; Tracy, K.; Krile, R.; Nishioka, M.; Taylor, M.; Riggs, K.; Stone, H. *Decontamination of Toxic Industrial Chemicals and Chemical Warfare Agents On Building*

Materials Using Chlorine Dioxide Fumigant and Liquid Oxidant Technologies; EPA: Columbus, OH, 2009.

(4) Richardt, A.; Blum, M. M., *Decontamination of Warfare Agents: Enzymatic Methods for the Removal of B/C Weapons*; Wiley-VCH: Weinheim, Germany, 2008.

(5) Hartleib, J.; Rüterjans, H. *Protein Expression Purif.* **2001**, *21* (1), 210–219.

(6) Blum, M.-M.; Löhr, F.; Richardt, A.; Rüterjans, H.; Chen, J. C. H. *J. Am. Chem. Soc.* **2007**, *128* (39), 12750–12757.

(7) Katesmi, V.; Lücke, C.; Koepke, J.; Löhr, F.; Maurer, S.; Fritzsche, G.; Rüterjans, H. *Biochemistry* **2005**, *44* (25), 9022–9033.

(8) Krajewska, B. *Enzyme Microb. Technol.* **2004**, *35* (2–3), 126–139.

(9) Lee, K.; Ki, C.; Baek, D.; Kang, G.; Ihm, D.-W.; Park, Y. *Fibers and Polymers* **2005**, *6* (3), 181–185.

(10) Pal, A.; Khanum, F. *Process Biochem.* **2011**, *46* (6), 1315–1322.

(11) Herricks, T. E.; Kim, S.-H.; Kim, J.; Li, D.; Kwak, J. H.; Grate, J. W.; Kim, S. H.; Xia, Y. *J. Mater. Chem.* **2005**, *15* (31), 3241.

(12) Wang, Z.-G.; Wan, L.-S.; Liu, Z.-M.; Huang, X.-J.; Xu, Z.-K. *J. Mol. Catal. B: Enzym.* **2009**, *56* (4), 189–195.

(13) Jia, H.; Zhu, G.; Vugrinovich, B.; Kataphinan, W.; Reneker, D. H.; Wang, P. *Biotechnol. Prog.* **2002**, *18* (5), 1027–1032.

(14) Wang, Y.; Hsieh, Y. L. *J. Membr. Sci.* **2008**, *309* (1–2), 73–81.

(15) Ye, P.; Xu, Z.-K.; Wu, J.; Innocent, C.; Seta, P. *Macromolecules* **2005**, *39* (3), 1041–1045.

(16) Ye, P.; Xu, Z.-K.; Wu, J.; Innocent, C.; Seta, P. *Biomaterials* **2006**, *27* (22), 4169–4176.

(17) Hwang, E. T.; Tatavarty, R.; Lee, H.; Kim, J.; Gu, M. B. *J. Mater. Chem.* **2011**, *21* (14), S215–S218.

(18) Kim, T. G.; Park, T. G. *Biotechnol. Prog.* **2006**, *22* (4), 1108–1113.

(19) Drevon, G. F.; Russell, A. J. *Biomacromolecules* **2000**, *1* (4), 571–576.

(20) Drevon, G. F.; Danielmeier, K.; Federspiel, W.; Stolz, D. B.; Wicks, D. A.; Yu, P. C.; Russell, A. J. *Biotechnol. Bioeng.* **2002**, *79* (7), 785–794.

(21) Filocamo, S.; Stote, R.; Ziegler, D.; Gibson, H. *J. Mater. Res.* **2011**, *26* (8), 1042–1051.

(22) Kim, J.; Grate, J. W.; Wang, P. *Chem. Eng. Sci.* **2006**, *61* (3), 1017–1026.

(23) Cao, L.; van Rantwijk, F.; Sheldon, R. A. *Org. Lett.* **2000**, *2* (10), 1361–1364.

(24) Kim, B. C.; Nair, S.; Kim, J.; Kwak, J. H.; Grate, J. W.; Kim, S. H.; Gu, M. B. *Nanotechnology* **2005**, *16* (7), S382.

(25) Wang, Y.; Hsieh, Y.-L. *J. Polym. Sci., Part A: Polym. Chem.* **2004**, *42* (17), 4289–4299.

(26) Xie, J.; Hsieh, Y.-L. *J. Mater. Sci.* **2003**, *38* (10), 2125–2133.

(27) Jiang, H.; Hu, Y.; Li, Y.; Zhao, P.; Zhu, K.; Chen, W. *J. Controlled Release* **2005**, *108* (2–3), 237–243.

(28) Han, D.; Boyce, S. T.; Steckl, A. J. *J. Mater. Res. Soc. Symp. Proc.* **2008**, *1094*, 1094–DD06–02.

(29) Han, D.; Steckl, A. J. *Langmuir* **2009**, *25* (16), 9454–9462.

(30) Bedford, N. M.; Steckl, A. J. *ACS Appl. Mater. Interfaces* **2010**, *2* (8), 2448–2455.

(31) Hoskin, F. C. G.; Walker, J. E.; Stote, R. *Chem.-Biol. Interact.* **1999**, *119*, 439–444.

(32) Hartleib, J.; Rüterjans, H. *Biochim. Biophys. Acta, Protein Struct. Mol. Enzymol.* **2001**, *1546* (2), 312–324.